



UNIVERSITY OF LEEDS

This is a repository copy of *Depolymerized RG-I enriched pectin from citrus segment membrane modulates gut microbiota, increases SCFAs production, promotes the growth of Bifidobacterium spp., Lactobacillus spp. and Faecalibaculum spp.*

White Rose Research Online URL for this paper:
<http://eprints.whiterose.ac.uk/153464/>

Version: Accepted Version

Article:

Mao, G, Li, S, Shen, X et al. (5 more authors) (2019) Depolymerized RG-I enriched pectin from citrus segment membrane modulates gut microbiota, increases SCFAs production, promotes the growth of Bifidobacterium spp., Lactobacillus spp. and Faecalibaculum spp. *Food & Function*, 10 (12). pp. 7828-7843. ISSN 2042-6496

<https://doi.org/10.1039/C9FO01534E>

This paper is protected by copyright. This is an author produced version of a paper published in *Food & Function*. Uploaded in accordance with the publisher's self-archiving policy.

Reuse

Items deposited in White Rose Research Online are protected by copyright, with all rights reserved unless indicated otherwise. They may be downloaded and/or printed for private study, or other acts as permitted by national copyright laws. The publisher or other rights holders may allow further reproduction and re-use of the full text version. This is indicated by the licence information on the White Rose Research Online record for the item.

Takedown

If you consider content in White Rose Research Online to be in breach of UK law, please notify us by emailing eprints@whiterose.ac.uk including the URL of the record and the reason for the withdrawal request.



eprints@whiterose.ac.uk
<https://eprints.whiterose.ac.uk/>

Food & Function

Linking the chemistry and physics of food with health and nutrition

Accepted Manuscript

This article can be cited before page numbers have been issued, to do this please use: G. Mao, S. Li, X. Shen, S. Zhou, C. Orfila, R. J. Linhardt, X. Ye and S. Chen, *Food Funct.*, 2019, DOI: 10.1039/C9FO01534E.



This is an Accepted Manuscript, which has been through the Royal Society of Chemistry peer review process and has been accepted for publication.

Accepted Manuscripts are published online shortly after acceptance, before technical editing, formatting and proof reading. Using this free service, authors can make their results available to the community, in citable form, before we publish the edited article. We will replace this Accepted Manuscript with the edited and formatted Advance Article as soon as it is available.

You can find more information about Accepted Manuscripts in the [Information for Authors](#).

Please note that technical editing may introduce minor changes to the text and/or graphics, which may alter content. The journal's standard [Terms & Conditions](#) and the [Ethical guidelines](#) still apply. In no event shall the Royal Society of Chemistry be held responsible for any errors or omissions in this Accepted Manuscript or any consequences arising from the use of any information it contains.

Depolymerized RG-I enriched pectin from citrus segment membrane modulates gut microbiota, increases SCFAs production, promotes the growth of *Bifidobacterium* spp., *Lactobacillus* spp. and *Faecalibaculum* spp.

Guizhu Mao¹, Shan Li⁶, Caroline Orfila⁵, Xuemin Shen¹, Shengyi Zhou¹, Robert J. Linhardt⁴, Xingqian Ye^{1, 3, 4}, Shiguo Chen^{1, 3, 4*}

¹ College of Biosystems Engineering and Food Science, National-Local Joint Engineering Laboratory of Intelligent Food Technology and Equipment, Zhejiang Key Laboratory for Agro-Food Processing, Zhejiang Engineering Laboratory of Food Technology and Equipment, Zhejiang University, Hangzhou 310058

² Fuli Institute of Food Science, Zhejiang University, Hangzhou 310058

³ Ningbo Research Institute, Zhejiang University, Hangzhou 315100

⁴ Center for Biotechnology and Interdisciplinary Studies, Rensselaer Polytechnic Institute, Troy, New York 12180, USA

⁵ School of Food Science and Nutrition, University of Leeds, Leeds LS2 9JT, United Kingdom

⁶ Institute of Nutrition and Health, Qingdao University, Qingdao 266071

*Corresponding author: Shiguo Chen, College of Biosystem Engineering and Food Science, Zhejiang University, Hangzhou 310058, China. E-mail: chenshiguo210@163.com; Tel: 86-0571-88982151.

Abstract:

Rhamnogalacturonan-I (RG-I) enriched pectin (WRP) was recovered from citrus processing water by sequential acid and alkaline treatment in a previous study. RG-I enriched pectin was proposed as a potential supplement for functional food and pharmaceutical development. However, previous studies illustrated favorable modulations of gut microbiota by RG-I enriched pectin were based on *in vitro*, changes in the overall microbial structure and whether there is a structure-dependent way in modulation of gut microbiota remain largely enigmatic. In the present study, modulations of gut microbiota by commercial pectin (CP), WRP and its depolymerized fraction (DWRP) with different RG-I content and Mw were compared *in vivo*. Revealed by 16s rRNA high-throughput sequencing, WRP and DWRP mainly composed of RG-I, modulated the gut microbiota in a positive way. WRP significantly increased the abundance of prebiotic such as *Bifidobacterium* spp., *Lactobacillus* spp., while DWRP increased SCFAs producers including species in Ruminococcaceae family. By maintaining more balanced gut microbiota composition and enriching some SCFA producers, dietary WRP and DWRP also elevated SCFAs content in the colon. Collectively, our findings offer new insight into structure-activity correlation of citrus pectin and provide impetus towards the development of RG-I enriched pectin with small molecular weight for specific use in health-promoting prebiotics ingredient and therapeutic.

Keywords: RG-I; citrus pectin; gut microbiota; SCFAs; prebiotic

1. Introduction

Canned citrus segments, as an instant and delicious fruit product, enjoying a great popularity all over the world with an annual trade value of almost \$900 million (source: UN Comtrade). China accounts for nearly 70% canned citrus segments on the international market, is the largest citrus planting and harvesting country in the world¹. However, up to one million pounds of solid waste and effluent water were produced in citrus canning processing factories annually, latter of which was actually segment membrane solution, contains high organic substances (polysaccharides principally), representing both an economic and an environmental challenge². Our previous study recovered pectin with higher RG-I content from basic water during the segment membrane removal process, occurring in citrus canning factories².

Pectin is mainly composed of structurally distinct regions including homogalacturonan (HG), rhamnogalacturonan (RG-I), rhamnogalacturnan (RG-II)³. HG, whose backbone consisted of α -1,4 linked galacturonic acid that is partially methyl-esterified at C-6 and *O*-acetylated in positions 2 and 3, occupying about 65% of commercial pectin. RG-I, accounting for 20-35% of commercial pectin, is based on a backbone being formed from a repeating disaccharide of $[\rightarrow 2)\text{-}\alpha\text{-L-Rhap-(1}\rightarrow 4)\text{-}\alpha\text{-D-GalAp-(1}\rightarrow]$ residues with neutral side chains attached to the O-4 position and sometimes the O-3 position of $\alpha\text{-L-Rhap}$ backbone units⁴. Extraction of commercial pectin uniformly aims at maintaining more HG content for best quality control and better application in the food industry as a gelling agent, thickening agent, stabilizer, emulsifier, and color-protecting agent⁵⁻⁷. However, during

the harsh extraction condition, RG-I region is mostly destroyed ⁸, which is gaining attention increasingly because of its bioactivity including anti-galectin-3 activity (a lectin associated with cancer progression and metastasis) ⁷, antitumor activity ⁹, immunomodulation ability ¹⁰, and prebiotic activity ^{11, 12}. Structure features including RG-I content, neutral sugar content, neutral side chains length and variable linking types, and molecular weight (Mw), determined to some extent the suitability of specific application of the pectin per se ^{5, 13}.

The structural diversity of pectin and the increasing concern in RG-I region arouse more people rethinking the relationship between pectin's structure and function recently. Gut microbiota plays fundamental roles in modulation of host's metabolism, nutrition and immunity ^{14, 15}. Gut microbiota impairment is tightly linked to various disease and metabolic disorders including inflammation bowel diseases ^{16, 17}, diabetes ^{18, 19}, non-alcoholic fatty liver disease (NAFLD) ²⁰, hypertension ²¹, obesity ^{22, 23}, and cardiovascular disease ^{23, 24}. Restoring the disrupted gut microbiota through personalized colonization of prebiotics represents an effective strategy for the management of gut microbiota-related diseases ^{25, 26}. Accumulating evidence illustrated that non-digestible carbohydrates in daily diet can alleviate and treat disease through modulating the gut microbiota composition ²⁷. Therefore, elucidating the effect of pectin as a dietary supplement on gut microbiota would be significantly beneficial to clarify its functional mechanisms. RG-I region is highly complex part of pectin and is reported to be potentially used as prebiotics and gastrointestinal drug delivery microcapsules ^{28, 29}. Previous studies reported that citrus pectin has *in vitro*

prebiotic activity by stimulating the growth of *Bifidobacterium bifidum*, *Lactobacillus paracasei*, *Bacteroides plebeius*, and *Ruminococcus gnavus* during *in vitro* fermentation^{12, 13, 30}. Besides, the favourable changes in microbiota composition after pectin supplementation depended greatly on RG-I content, neutral sugars composition, degree of esterification and branching¹³. However, the structure-function relationship of pectin has few been evaluated *in vivo* before.

Considering the remarkable non-digestibility of citrus pectin in the upper gastrointestinal tract^{12, 31, 32}, we investigated the relationship between structure of pectin and modulation of gut microbiota *in vivo*. In our study, the basic structure and chain conformation of CP, WRP, and DWRP were investigated by NMR, SEC-MALLS and AFM. C57BL/6J mice were administrated with CP, WRP and DWRP at a dosage of 100mg/kg/day, their effects on gut microbiota composition and SCFAs were studied by 16S rRNA and gas chromatography (GC). The diversity and composition of gut microbiota were compared at the phylum, class, family and genus levels. Meanwhile, the spatial structure difference of gut microbiota was also involved. Our study indicates distinct modulations of gut microbiota by different pectin and provides theoretical foundations for developing RG-I enriched pectin as a health-promoting and therapeutic prebiotics ingredient.

2 Materials and Methods

2.1 Material and preparation of pectin

Citrus segments material (*Citrus unshiu Marc.*) recovered from canning processing basic water was provided by a citrus fruit canning factory in China. The

material was washed with 95% (v/v) food grade ethanol for 2-3 times to desalt, the pectin was precipitated and oven-dried at 55°C for 24-36h, which was abbreviated as WRP. DWRP was degraded from WRP based on the metal-free Fenton reaction, relying on H₂O₂/ascorbic acid, adapted from a previous study³³. Briefly, the reaction conditions were 200 mM H₂O₂, 20 mM ascorbic acid and temperature at 45°C. The WRP (5000mg) starting material was dissolved in 1000 mL ultrapure water, H₂O₂ and ascorbic acid was then added with mixing and the reaction was maintained at 45°C for 30min. The depolymerized products were desalted by dialysis using a 500 Da cut-off membrane for 72h under flowing water, concentrated and subsequently lyophilized to obtain refined samples for further study.

2.2 Structural analysis of pectin

2.2.1 Primary structure of CP, WRP, and DWRP

Primary structure of the three pectin was studied by HPLC, FTIR, and NMR. Monosaccharide standards, 1-phenyl-3-methyl-5-pyrazolone (PMP), D₂O and commercial pectin from citrus peel (abbreviated as CP) were all purchased from Sigma-Aldrich (Shanghai, China). All other used chemicals were of analytical grade. Chemical compositions of CP, WRP and DWRP (Table 1) were determined according to previous described methods with modifications³⁴. FTIR and NMR analysis were conducted based on the method of a previous report⁸.

2.2.2 Chain conformation of CP, WRP, and DWRP

Chain conformation of the three pectin was studied by SEC-MALLS and AFM. For size exclusion chromatography with multi-angle laser light scattering

(SEC-MALLS) analysis, pectin was dissolved in 0.2M NaCl solution at a concentration of 5mg/mL. 50 μ L of solution was injected through a sample loop after filtering through a syringe-filter (pore size of member was 0.22 μ m). The molar mass and root mean square (RMS) radius of gyration was determined through high-performance (HP) size exclusion chromatography (SEC) equipped with multi-angle laser light scattering (MALLS) (Wyatt Dawn Heleos-II, USA) and RI detector at 25 °C. Isocratic elution with 0.2M NaCl solution at a flow rate of 0.5mL/min was performed on combined columns including Shodex OH SB-G (pre-column), Shodex SB-806 HQ and Shodex SB-804 HQ (Showa Denko KK, Japan). The molar mass was calculated based on the dn/dc value of 0.0880mL/g.

For atomic force microscope (AFM) analysis, pectin was dissolved in ultrapure water at a concentration of 1mg/mL with continuous stirring for 2 h incubating at 60°C. The stock solutions were next diluted by sodium dodecyl sulphate (SDS) solution, obtaining a mixed solution containing pectin and SDS both at a concentration of 10 μ g/mL. The diluted solutions were then stirred for 24h and filtered through a syringe-filter (pore size of member was 0.22 μ m). After the samples were ready, 10 μ L pectin solution was moved to three freshly cleaved mica substrates using micropipette respectively. Then three mica substrates were air-dried and observed by AFM (XE-70, Park Scientific Instruments, Suwon, Korea) using tapping mode in air at room temperature (humidity: 50%-60%). The probe is a classical silicon cantilever (Appnano AN-NSC10) with a spring constant of 37N/M and a resonance frequency of approximately 300 kHz. Nanoscope Analysis software was

used for image manipulation.

View Article Online
DOI: 10.1039/C9FO01534E

2.3 Animals and experimental design

All procedures were approved by the Institutional Animal Care and Use Committee of Zhejiang University School of Medicine. 40 C57BL/6J male mice (SPF, 6-8 weeks old, IACUC-20180917-02) were purchased from Zhejiang Chinese Medical University Laboratory Animal Research Center. The mice were kept under the specific-pathogen-free conditions in a 12-hour light/dark cycle with free access to food and sterile drinking water (DW) in a temperature-controlled room ($21^{\circ}\text{C}\pm 2^{\circ}\text{C}$). Before starting the experiments, the mice were housed 25 per cage and exchanged multiple times to make fecal microbiomes homogeneous. After one week of acclimatization, the mice were randomly divided into four groups: CD group, CD-CP group, CD-WRP group and CD-DWRP group (10 mice per group, 5 mice per cage) and fed for 9 weeks with standard chow diet (Rodent diet, SHOBREE, Jiangsu Synergy Pharmaceutical Biological Engineering Co, Ltd, Nanjing China). Mice were supplemented daily with 200 μL of sterile water (vehicle), CP (100mg/kg·d), WRP (100mg/kg·d) or DWRP (100mg/kg·d) respectively via intragastric gavage. The compositions and energy densities of the diets are listed in Table S2. The body weight was measured weekly, food intake was daily recorded. At the time indicated, the mice were fasting for 12 hours and anaesthetised, the whole blood was collected from the orbital plexus. Then, the mice were sacrificed. Epididymal white adipose tissues, liver, small intestine, caecum and colon samples were removed and weighed. Meanwhile, caecal contents were collected in Eppendorf tubes and immediately

stored at -80°C for subsequent analysis. The intestinal tissue index was calculated using the following formula: intestinal tissue index = intestinal tissue weight/body weight.

2.4 Biochemical analysis and cytokine measurements of serum

Serum was isolated by centrifugation (4°C , 12,000g, 10min). Serum total cholesterol and triacylglycerol concentrations were determined using commercial kits (Nanjing Jiancheng Bioengineering Institute, Nanjing, China) according to the manufacturer's instructions. TNF- α , LPS and insulin levels were then quantified using commercial ELISA kits (Cloud-clone Crop, USA).

2.5 16S rDNA analysis

Five samples of each group were selected randomly for 16S rRNA analysis. DNA was extracted from the caecal solid contents of mice by using the E.Z.N.A.® Stool DNA Kit (D4015, Omega, Inc., USA) according to manufacturer's instructions. The total DNA was eluted in 50 μL of Elution buffer and stored at -80°C until measurement in the PCR by LC-Bio Technology Co., Ltd. The V3-V4 region of the prokaryotic (bacterial and archaeal) small-subunit (16S) rRNA gene was amplified with slightly modified versions of primers 338F ($5^{\prime}\text{-ACTCCTACGGGAGCAGCAG-3}^{\prime}$) and 806R ($5^{\prime}\text{-GGACTACHVGGGTWTCTAAT-3}^{\prime}$)³⁵. The 5' ends of the primers were tagged with specific barcodes per sample and sequencing universal primers.

The PCR products were purified by AMPure XT beads (Beckman Coulter Genomics, Danvers, MA, USA) and quantified by Qubit (Invitrogen, USA). The

amplicon pools were prepared for sequencing and the size and quantity of the amplicon library were assessed on Agilent 2100 Bioanalyzer (Agilent, USA) and with the Library Quantification Kit for Illumina (Kapa Biosciences, Woburn, MA, USA), respectively. PhiX Control library (v3) (Illumina) was combined with the amplicon library (expected at 30%). The libraries were sequenced either on 300PE MiSeq runs and one library was sequenced with both protocols using the standard Illumina sequencing primers, eliminating the need for a third (or fourth) index read.

Samples were sequenced on an Illumina MiSeq platform according to the manufacturer's recommendations, provided by LC-Bio. Paired-end reads was assigned to samples based on their unique barcode and truncated by cutting off the barcode and primer sequence. Paired-end reads were merged using FLASH. Quality filtering on the raw tags were performed under specific filtering conditions to obtain the high-quality clean tags according to the FastQC (V 0.10.1). Chimeric sequences were filtered using Verseach software (v2.3.4). Sequences with $\geq 27\%$ similarity were assigned to the same operational taxonomic units (OTUs) by Verseach (v2.3.4). Representative sequences were chosen for each OTU, and taxonomic data were then assigned to each representative sequence using the RDP (Ribosomal Database Project) classifier. The differences of the dominant species in different groups, multiple sequence alignment were conducted using the PyNAST software to study phylogenetic relationship of different OTUs. OTUs abundance information were normalized using a standard of sequence number corresponding to the sample with the least sequences. Alpha diversity is applied in analyzing complexity of species

diversity for a sample through 4 indices, including Chao1, Shannon, Simpson and Observed species. All these indices in our samples were calculated with QIIME (Version 1.8.0). Beta diversity analysis was used to evaluate differences of samples in species complexity. Beta diversity was calculated by principle co-ordinates analysis (PCoA) and cluster analysis by QIIME software (Version 1.8.0). The Spearman's rho nonparametric correlations between the gut microbiota and heal-related indexes were determined using R packages (V2.15.3).

2.6 Caecal and colonic short-chain fatty acids

Short-chain fatty acids (SCFAs), including acetate, propionate and butyrate, were measured in caecal and colonic samples using an external standard method described by Wu T R et al.³⁶ with minor modifications. Briefly, caecal contents (70mg) of each animal were suspended in 700µL 0.01M of PBS, and mixed intermittently on a vortex mixer for 10 min and then centrifuged at 12,000g for 5min at 4°C. The supernatant was acidified with an equal volume of 0.1M H₂SO₄ and extracted with 800µL of ethyl ether. The contents of SCFAs were measured in the organic phase using a gas chromatograph (Agilent Technologies, Stockport, UK) equipped with a 30m×0.25mm×0.25µm HP-INNOWax column (No. 19091N-133; Agilent Technologies, USA) and flame ionization detector (Agilent Technologies). The determination program for SCFAs was as follows: the temperatures of injector and detector were 240°C and the column temperature was 200°C. Split injection (20:1). The initial column temperature was 110°C and maintained for 5 min, thereafter increasing at a rate of 20°C/min until reaching 240°C, which was held there for 5 min.

The flow rates of N₂ (carrier gas), H₂ (make-up gas), and air were 20, 15 and 150 mL min⁻¹, respectively. SCFAs of all samples were quantified by comparing peak areas with those of chemical standards.

View Article Online
DOI: 10.1039/C9FO01534E

2.8 Statistical analysis

Data were expressed as means \pm SD. Statistical analysis was performed using GraphPad Prism V.7.04 (GraphPad Software, USA). One-way analysis of variance (ANOVA) for multiple comparisons followed by the non-parametric Kruskal-Wallis test with Dunnett's multiple comparisons test. Significance was set at $p < 0.05$.

3 Results and discussion

3.1 Pectin structure analysis

CP, WRP and DWRP are mainly composed of galacturonic acid, rhamnose, galactan, arabinan, glucuronic acid, fucose, glucose (Table 1), in different proportions. CP has the highest HG content (55.22%), followed by DWRP (42.29%) and WRP (25.03%). Conversely, WRP has the highest RG-I content (70.44%), followed by DWRP (56.29%) and CP (35.77%). WRP has the highest degree of branching with a Rha:[Gal+Ara] ratio of around 1:20, the branches dominated by arabinan, while CP and DWRP has lower arabinan. Despite the differences in HG/RGI content, CP and WRP both have similarly large Mw of around 500 kDa (Table S1), while DWRP has low Mw of 12.1 kDa (Fig. S1). According to FTIR (Fig. 1A), both CP and DWRP gave an obvious absorbance at 1745 cm⁻¹ (COO-R) and 1635 cm⁻¹ (COO-), only the WRP showed an sole absorption peak at 1635 cm⁻¹, confirming that WRP had the highest RG-I content. Detailed structural information

about the proton environment of CP, WRP and DWRP was shown by ^1H NMR (Fig. 1B). Five major signals were assigned to the proton in the D-galacturonic acid: H-1, 5.03 ppm; H-2, 3.66 ppm; H-3, 3.93 ppm; H-4, 4.07 ppm and H-5, 4.35 ppm, respectively³⁷. In the anomeric region, the signal at 5.03 ppm was attributed to the H-1 of rhamnose⁹, which was obvious in both spectra of WRP and DWRP. Besides, the signals between 5.07 and 5.20 ppm were attributed to the H-1 of different types of arabinan⁸. Therefore, CP, DWRP and WRP were shown to have successively larger signals for arabinan, consistent with the monosaccharide composition. Besides, the spectra from WRP and DWRP showed additional peaks that were hard to assign, probably owing to the presence of larger Ara, Gal, and Rha amounts, nearly equal to that of GalA.

SEC is most appropriate for macromolecules with large Mw. Conformation plots of CP and WRP in 0.2M aqueous NaCl solution are calculated from the slope between RMS radius and molar mass (Fig. 2A). The slope value of linear fitting for CP and WRP was 0.12 and 0.05 respectively, predicting branched conformation consistent with the anomalous SEC phenomenon of plots bending upward at the low molar mass region^{38, 39}. Mark-Houwink-Sakurada equation (MHS, $[\eta]=\text{KMw}^\alpha$) was used to infer the chain conformation of macromolecules⁴⁰. Value for CP and WRP was $[\eta]=0.22\text{Mw}^{0.61}$ (mL/g), $[\eta]=0.58\text{Mw}^{0.45}$ (mL/g) respectively (Fig. 2B). According to the literature, values of α ranging from 0-0.3, 0.5-0.8, 1 and 1.8-2 correspond to chain conformation is spherical, random coil, semi-rigid chain and rod chain respectively^{38, 41}. CP and WRP had α values of 0.61 and 0.45 respectively, indicating a higher

branched chain structure of WRP.

AFM was used to imagine the molecule shapes of CP, WRP and DWRP (Fig. 2). The micrographs show that chain-like structure is characteristic for all the pectins. WRP appears significantly more branched than CP and DWRP, with interlaced structure of a network. CP and DWRP were shown to have successively higher linear and sparse branch compared to WRP, consistent with the chromatograms of the chain conformation. The expected diameters of single polysaccharide strands, imaged by AFM and adopting helical conformations, range from 0.5 to 0.8 nm⁴². The diameters of CP, WRP and DWRP were calculated as 0.58 nm, 0.75 nm and 1 nm respectively, suggesting that DWRP is probably slightly aggregated.

3.2 Effects of pectin with different RG-I content on the structure of gut microbiota community

RG-I region can be partially degraded by specific gut microbes including including *Bacteroides thetaiotaomicron*, *Bifidobacterium Longum*,⁴³. Nevertheless, the effect of RG-I on the composition and diversity of the gut microbiota *in vivo* is unknown. We investigated and compared the effects of pectin differing in RG-I content, Mw and conformation on the gut microbiota profile in mice.

C57BL/6J mice underwent a nine-week dietary treatment consisting of conventional chow supplemented with the three pectin preparations. High-throughput sequencing was adopted to characterize the diversity of caecal microbiota at the end of the nine week intervention. Surprisingly, the caecal gut community richness and diversity after the interventions with large Mw pectins (CD-CP and CD-WRP) were

not significantly different from the standard chow (CD), as demonstrated by Chao1, Shannon and Simpson (Table S3). The CD-DWRP significantly decrease the richness and diversity of caecal microbiota. In accordance with our observation, oral administration of *Lentinula edodes*-derived polysaccharides also significantly decreases diversity and the amount of OTUs (Operation Taxonomic Units) in caecal microbiota⁴⁴. As for RG-I enriched pectin (Fig S3.), we tentatively put forward that this was probably owing to the relative enrichment effects of some beneficial bacteria while the destructive bacterial was reduced because of its antibacterial effects, which was proposed by the previous studies^{30, 45-47}. Nevertheless, the exact explanation needs further analysis of detail on specific microbial species.

Based on clustering analysis (Fig S2), supplementation with pectins led to change in the cluster of microbial groups compared to standard chow. The groups were further analysed and compared using principal component analysis (PCA) and 3D-principal coordinate analysis (3D-PCoA). As shown by PCA, the three pectin changed the structure of the gut microbiota dissimilarly (Figure 3). With a greater distinction in segregation, 3D-PCoA depicted that CD-WRP group showed a more pronounced microbiota structural shift than that of CD-CP and CD-DWRP groups all along the first, second, and third principle (Figure 3b), compared to CD alone. This suggests a strong effect of arabinan-rich RG-I pectin on the microbiome. A similar microbiota community modulation pattern was observed in response to CD-CP and CD-DWRP (Figure 3b). They both have lower RG-I content and branching. Overall, the results suggest that structure (Mw, branching) and composition

(RG-I/HG/arabinose content) of pectin are important factors in the modulation of gut microbiota in C57BL/6J mice.

View Article Online
DOI: 10.1039/C9FO01534E

Bacterial populations of all four diet groups were then compared at the phylum, class and genus levels (Fig. 4). At the phylum level, the dominant bacterial communities were Firmicutes and Bacteroidetes (Fig. 4A). The Bacteroidetes group is a major group responsible for polysaccharide degradation, while the Firmicutes group possess smaller number of polysaccharides-degrading enzymes⁴⁸. In addition, WRP and DWRP were found to have a differing effect on the abundance of Actinobacteria (Fig. 4A). WRP decreased the abundance of Actinobacteria significantly, which was increased by DWRP and even higher than the CD group.

At the class level, the dominant bacterial were classified into Clostridia, Bacteroidia, Deltaproteobacteria and Actinobacteria, with a less proportion of Erysipelotrichia, Bacilli and Epsilonproteobacteria (Fig. 4B). At the genus level, the dominant bacterial were classified into *Porphyromonadaceae*, *Desulfovibrio*, *Lachnospiraceae*, *Lachnoclostridium*, *Bacteroides*, *Ruminococcaceae*, *Lactobacillus* and *Oscillospira* (Fig. 4C). To a lesser proportion, *Butyrivibrio*, *Ruminococcus*, *Acetatifactor*, *Olsenella* and *Allobaculum* were also found in different proportions in these four groups (Fig. 4C).

3.3 Key phlotypes of gut microbiota modulated by supplementation of chow with WRP and DWRP

To identify the specific bacteria that were modulated in response to different pectin, the linear discriminant analysis (LDA) effect size (LEFse) analysis was

performed. The taxonomic cladogram and LDA score obtained from LEFSe analysis identified and visualized the modulatory effect of CP, WRP and DWRP on caecal microbiota (Fig 5, Fig 6 and Fig S4). At the genus level, a pairwise comparison between the caecal microbiota of the CD-CP, CD-WRP and CD-DWRP groups displayed that, WRP treatment significantly promoted the growth of *Bacteroides spp.* and its next-generation such as *Bacteroides caecimuris*, *Bacteroides ovatus*, Ruminococcaceae family, especially its next-generation such as *Ruminococcus spp.*, *Butyricicoccus spp.* in caecal microbiota of C57BL/6J mice, while DWRP significantly increase the abundance of *Bifidobacterium spp.*, *Lactobacillus spp.*, *Faecalibaculum spp.*, *Faecalibaculum rodentium*, and *Bacteroides thetaiotaomicron*. (Fig 6).

Specifically, DWRP treatment increased the amount of *Bifidobacterium spp.* and *Lactobacillus spp.* by about 3 to 8 fold compared to other three groups (Table 2). The amount of *Faecalibaculum spp.* in CD-DWRP group was increased by 17 to 35 fold compared to other two pectin treated groups. Similarly, the amount of *Ruminococcus spp.* in CD-WRP group was also significantly increased by 5 fold compared to the CD group. As for the family level, WRP treatment significantly promoted the growth of Ruminococcaceae family, Desulfovibrionaceae family and Bacteroidales family, while the DWRP treatment significantly increased the abundance of Clostridiales family, Erysipelotrichaceae family and Coriobacteriaceae family (Fig. 5 and Fig 6). More specifically, the amount of Ruminococcaceae family was increased by 16 fold in CD-WRP group compared to the CD group (Table 2). As for the class level, the CP

and DWRP showed significant increase in the abundance of Deltaproteobacteria and Actinobacteria, Erysipelotrichia respectively, when the CD-WRP group showed insignificant decreased abundance of them (Fig. 4). However, at the phylum level, only the Actinobacteria was discovered to be increased by DWRP, no significant change in the phylum structure of caecal microbiota was found after CP or WRP intervention (Fig 4 and Fig S4). WRP and DWRP have a more specific and potentially beneficial effect on the caecal microbiota compared to CP, though they resulted in discrepant modulations of gut microbiota.

Ruminococcaceae family is one of autochthonous and benign species that reside in the caecum and the colon ⁴⁹. As short chain fatty acids (SCFAs) producer, it has been clarified to be responsible for the degradation of various polysaccharides ⁵⁰⁻⁵³. In the CD-WRP group, Ruminococcaceae family was significantly increased, whose population size is inversely correlated with increased intestinal permeability ⁵⁴, high blood triglycerides ⁵⁵ and obesity ⁵³. Among the Ruminococcaceae family, *Ruminococcus spp.* and *Butyricoccus spp.* were significantly enriched. *Ruminococcus spp.*, whose fermentation metabolites is acetate, was also reported to be enriched by oral administration of established prebiotics like inulin ⁵⁶. *Butyricoccus spp.*, with butyrate-producing activity, has been reported to be a beneficial bacterial that can suppress inflammatory related diseases ⁵⁷. Members in *Bacteroides spp.* can utilize nearly all of the major plant glycans including the most complex RG-I and RG-II region ^{58, 59}. Especially, the *Bacteroides thetaiotaomicron* was elucidated to have a large RGI-PUL (polysaccharide utilization location) and

galacturan-PUL thus can utilize RG-I backbone and galacturan side chains⁵⁸.

Furthermore, 60% of the *Bacteroides* spp. are capable of degrading arabinan side chains in RG-I region⁶⁰. Therefore, the average abundance of *Bacteroides* spp. is successively higher in the caecal samples from mice supplemented with CP, WRP and DWRP with sequentially higher RG-I and arabinan side chain content (Table 2). *Desulfovibrio* spp. was decreased in obese host^{61, 62}, *Clostridium_XIVa* spp. was enriched in the healthy mice compared to tumor-bearing mice⁶³. Since dietary WRP significantly increased the amount of *Desulfovibrio* spp. and *Clostridium_XIVa* spp., further studies are subsequently preferred to explore whether oral administration of WRP could be beneficial for ameliorating obesity or colon cancer.

As the main prebiotics, *Bifidobacterium* and *Lactobacillus* are both crucial for the maintenance of healthy homeostasis⁶⁴. DWRP significantly enriched *Bifidobacterium* and *Lactobacillus*, which was consistent to the previous research where the pectin fraction (with low Mw of 3000-4000Da) degraded from the parent citrus pectin showed much better prebiotic activity³². This could be due to increased solubility or accessibility of pectic backbone (due to less branches) to microbial degrading enzymes. Besides, *Faecalibaculum rodentium*, as a potentially important species, was also significantly enriched by DWRP (Table 2). It has higher fermentation ability, especially for butyrate production, is hypothesized as the main replacer of *Lactobacillus* and *Bifidobacterium* between the early and late stages of life, along with a shift from lactate metabolism to increased SCFAs production and carbohydrate metabolism⁶⁵.

Totally, oral administration of DWRP rather than CP or WRP enriched the amount of prebiotic microbiota. In another previous study, six pectic oligosaccharides standing for specific substructure within pectin and the parent polysaccharides were evaluated for the fermentation properties⁶⁶. Neutral sugar fractions was discovered to lead to an increase in *Bifidobacterium* populations and higher organic acid yields. Besides, arabinan, galactan, oligoarabinosides and oligogalactosides were the most selective substrates for bifidobacteria. Collectively, pectin with low Mw and higher neutral sugars content better promotes growth of beneficial bacteria^{66, 67}. Therefore, the prebiotic activity of DWRP is probably owing to its high RG-I content and low Mw.

3.4 Effects of citrus pectin with different RG-I content on SCFAs

SCFAs are end products of fermentation of dietary fibres by specific anaerobic intestinal microbiota^{68, 69}. Accumulating evidence suggests that SCFAs plays a crucial and favourable role in host physiology and energy homeostasis^{70, 71}. Acetate, propionate and butyrate are the most abundant components of SCFAs (constitute >95% of the SCFA content), while formate, caproate and valerate are present in substantially lower amounts and make up the remaining <5%⁷².

In the current study, the level of total SCFAs was found higher in both cecum and feces of CD-WRP and CD-DWRP group compared with the CD group, while that of CD-CP group was higher in cecum but slightly lower in feces (Fig. 7). It was in line with that some polysaccharides was reported to increase SCFAs production both *in vivo* and *in vitro*⁷³⁻⁷⁶, indicating that the gut-derived SCFAs together with gut

microbiota modulation may contribute to the beneficial effects of WRP and DWRP.

The CD-CP group contained significantly higher concentrations of acetate ($30.32 \pm 3.23 \mu\text{mol/g}$) and total SCFAs ($41.49 \pm 12.24 \mu\text{mol/g}$) compared to the CD group with acetate concentration of $12.51 \pm 2.46 \mu\text{mol/g}$ and total SCFAs concentration of $26.68 \pm 4.52 \mu\text{mol/g}$ in the caecal (Fig. 7A, Table S4), while this trend was surprisingly reverse in the colon (Fig. 7B). The production of acetate and butyrate were reported being promoted by the fermentation of galacturonic acid and xylose, while the production of propionate being promoted by arabinose and glucose fermentation⁷⁷. Collectively, the increase of acetate and butyrate in cecum might be due to the fermentation of GalA in CP. Interestingly, CD-WRP and CD-DWRP group showed no significant concentration increase in neither total SCFAs nor any kind of SCFAs in the caecal content, while the CD-WRP group significantly increased the concentrations of total SCFAs ($28.35 \pm 4.65 \mu\text{mol/g}$) and acetate ($20.57 \pm 2.09 \mu\text{mol/g}$) compared to the CD group with total SCFAs concentration of $20.43 \pm 2.09 \mu\text{mol/g}$ and acetate concentration of $13.69 \pm 1.58 \mu\text{mol/g}$ in the colonic content (Fig. 7B, Table S5). The slight increase production of propionate in CD-WRP and CD-DWRP was mainly owing to the fermentation of relatively higher content of Rha and other neutral sugars in RG-I¹³, which was also proved by the strong correlation between *Bacteroides* spp. and propionate content in caecum (Fig. S6). However, the SCFAs in the colonic content seemed to be successively not affected by CP and DWRP, which may be owing to the amount of CP and DWRP reaching the colon is lower.

Therefore, we tentatively presumed that there were a sequential degradative

model of pectin enriched with different region in the lower digestive tract, which was consistent with what was previously pointed out for complex glycan and arabinogalactan depolymerisation⁵⁹. It's possible that the RG-I enriched pectin with large Mw (WRP as a typical representative), arabinose and galacturonan side chains in RG-I region were firstly fermented in the cecum, the remaining RG-I fraction was then transferred to the colon and fermented subsequently; for the HG enriched pectin with high Mw and limited side chains content (CP as a typical representative), cecum was the main fermentation place, few could reach the colon; for pectin with relatively higher RG-I content and lower Mw (DWRP as a typical representative), partly could be fermented in cecum, while some could reach the colon.

3.5 Growth performance and biochemical parameters in response to dietary WRP and DWRP supplementation

After a 9-week of intervention, three pectin intervention groups all had a lower body weight and body weight gain than the CD group (Fig. 8B). Additionally, weight gain of CD-WRP group was the lowest. As indicated in previous study, dietary polysaccharides with a prebiotic effect was capable of decreasing the body weight as well as food intake of experimental mice^{69, 78}. Here dietary CP, WRP and DWRP were found to significantly decrease the body weight gain while no significant change in the food intake was discovered during four mice groups (Fig. S5). Differing from the fucoidan which was reported to lose weight by promoting satiety⁷⁹, both CD-WRP and CD-DWRP had similar average food intake with CD group, therefore weight gain decrease was not owing to energy intake reduction. Besides, pectin can

delay gastric emptying, slow the intestinal transport, affects the mixing of food and digestive enzymes, therefore affects the digestion and absorption of carbohydrates and fats ⁸⁰. Given that characteristic bacterial in lean host such as *Desulfovibrio* spp., *Bifidobacterium* spp. and *Clostridium_XIVa* spp. were largely enriched in WRP and DWRP, besides elevated concentrations of SCFAs could regulate energy homeostasis, the weight loss in these two group could be partly owing to that WRP and DWRP both stimulates beneficial gut microbiota especially for SCFA-producing ones and increases levels of total SCFAs in the colon.

Considering there is a tight correlation between SCFAs and mediation of inflammation and energy metabolism ⁶⁹, the levels of lipid and inflammatory cytokines from all mice were analysed (Table S6). Significant decrease of inflammatory cytokines levels including lipopolysaccharides (LPS) and Tumor Necrosis Factor- α (TNF- α) were found in both CD-WRP and CD-DWRP group (Table S6). The discrepancy occurred here between three groups was probably owing to the discriminating modulation of gut microbiota resulting from different structural features (Fig. 3B; Fig. 4). Since when LPS is absorbed and enters into circulation system, the inflammatory response of the host will be triggered ⁸¹. Therefore, taken together, the prebiotic activity by RG-I enriched DWRP in C57BL/6J mice is mainly mediated by marked structure modulation of the gut microbiota, which includes inhibiting a wide range of intestinal microbes and enriching some SCFA producers, and at least in part, by elevating SCFAs levels in the colon as well as reducing serum LPS levels.

4. Conclusion

By enriching the amount of prebiotic bacteria including *Bifidobacterium* spp., *Lactobacillus* spp., and SCFAs producing bacteria: *Faecalibacterium* spp., dietary DWRP shows best potential prebiotic effect. Whereas dietary WRP mainly enriched SCFAs producing bacteria including Ruminococcaceae family, especially *Ruminococcus* spp., *Butyrivibrio* spp. as well as *Bacteroides* spp. which is mainly responsible for arabinan side chains degradation. WRP and DWRP modulate the gut microbiota beneficial for the host in a structure-dependent path. Collectively, high RG-I content, low Mw will benefit the intestinal microbial ecology more. Besides, CD-WRP group showed the most pronounced caecal microbiota structural shift compared to the CD group, demonstrating a strong effect of arabinan-rich RG-I pectin on the modulation of caecal microbiota. Besides, based on the comparison of specific SCFAs in caecum and colon, we tentatively hypothesize that WRP were probably being sequentially utilized in the caecum and colon, while CP were mainly fermented in the caecum. By providing new insights into the well-admitted beneficial effects of RG-I enriched pectin in positive modulation of gut microbiota, our results rationalize that the RG-I enriched pectin with low Mw could be commercially used as a novel prebiotic substrate through manipulating the gut microbiota.

Conflicts of interest

There are no conflicts of interest to declare.

Author contributions

G.Z.M. designed experiments, performed the animal studies and statistical analysis and wrote the manuscript, S.G.C. and X.Q.Y. provided the funding and insightful suggestions to the work. S.L. helped to take care of the animals and performed the OGTT. C. O. and R.J.L. improved the language of this manuscript. All authors read and approved the final manuscript.

Acknowledgement

This work was financially supported in part by National Key R&D Program of China (2017YFE0122300 190) and National Fund (3187181559)

Reference

1. D. Wu, Y. Cao, J. Chen, H. Gao, X. Ye, D. Liu and S. Chen, Feasibility study on water reclamation from the sorting/grading operation in mandarin orange canning production, *Journal of Cleaner Production*, 2016, **113**, 224-230.
2. J. Chen, H. Cheng, D. Wu, R. J. Linhardt, Z. Zhi, L. Yan, S. Chen and X. Ye, Green recovery of pectic polysaccharides from citrus canning processing water, *Journal of Cleaner Production*, 2017, **144**, 459-469.
3. D. Mohnen, Pectin structure and biosynthesis, *Curr Opin Plant Biol*, 2008, **11**, 266-277.
4. F. Buffetto, V. Cornuault, M. G. Rydahl, D. Ropartz, C. Alvarado, V. Echasserieau, S. Le Gall, B. Bouchet, O. Tranquet, Y. Verhertbruggen, W. G. Willats, J. P. Knox, M. C. Ralet and F. Guillon, The Deconstruction of Pectic Rhamnogalacturonan I Unmasks the Occurrence of a Novel Arabinogalactan Oligosaccharide Epitope, *Plant Cell Physiol*, 2015, **56**, 2181-2196.
5. A. Noreen, Z. I. Nazli, J. Akram, I. Rasul, A. Mansha, N. Yaqoob, R. Iqbal, S. Tabasum, M. Zuber and K. M. Zia, Pectins functionalized biomaterials; a new viable approach for biomedical applications: A review, *Int J Biol Macromol*, 2017, **101**, 254-272.
6. E. D. Ngouémazong, S. Christiaens, A. Shpigelman, A. Van Loey and M. Hendrickx, The Emulsifying and Emulsion-Stabilizing Properties of Pectin: A Review, *Comprehensive Reviews in Food Science and Food Safety*, 2015, **14**, 705-718.
7. T. Zhang, Y. Lan, Y. Zheng, F. Liu, D. Zhao, K. H. Mayo, Y. Zhou and G. Tai, Identification of the bioactive components from pH-modified citrus pectin and their inhibitory effects on galectin-3 function, *Food Hydrocolloids*, 2016, **58**, 113-119.
8. H. Zhang, J. Chen, J. Li, L. Yan, S. Li, X. Ye, D. Liu, T. Ding, R. J. Linhardt, C. Orfila and S. Chen, Extraction and characterization of RG-I enriched pectic polysaccharides from mandarin citrus peel, *Food Hydrocolloids*, 2018, **79**, 579-586.
9. Z. Zhi, J. Chen, S. Li, W. Wang, R. Huang, D. Liu, T. Ding, R. J. Linhardt, S. Chen and X. Ye, Fast preparation of RG-I enriched ultra-low molecular weight pectin by an ultrasound accelerated Fenton process, *Sci Rep*, 2017, **7**, 541.
10. M. Meijerink, C. Rosch, N. Taverne, K. Venema, H. Gruppen, H. A. Schols and J. M. Wells, Structure Dependent-Immunomodulation by Sugar Beet Arabinans via a SYK Tyrosine Kinase-Dependent Signaling Pathway, *Front Immunol*, 2018, **9**, 1972.
11. N. Khodaei, B. Fernandez, I. Fliss and S. Karboune, Digestibility and prebiotic properties of potato rhamnogalacturonan I polysaccharide and its galactose-rich oligosaccharides/oligomers, *Carbohydr Polym*, 2016, **136**, 1074-1084.
12. A. Ferreira-Lazarte, F. J. Moreno, C. Cueva, I. Gil-Sanchez and M. Villamiel, Behaviour of citrus pectin during its gastrointestinal digestion and fermentation in a dynamic simulator (simgi(R)), *Carbohydr Polym*, 2019, **207**, 382-390.
13. N. Larsen, C. Bussolo de Souza, L. Krych, T. Barbosa Cahu, M. Wiese, W. Kot, K. M. Hansen, A. Blennow, K. Venema and L. Jespersen, Potential of Pectins to Beneficially Modulate the Gut Microbiota Depends on Their Structural Properties, *Front Microbiol*, 2019, **10**, 223.
14. F. Sommer and F. Backhed, The gut microbiota--masters of host development and physiology, *Nat Rev Microbiol*, 2013, **11**, 227-238.
15. A. Heintz-Buschart and P. Wilmes, Human Gut Microbiome: Function Matters, *Trends*

- Microbiol*, 2018, **26**, 563-574.
16. K. Matsuoka and T. Kanai, The gut microbiota and inflammatory bowel disease, *Semin Immunopathol*, 2015, **37**, 47-55.
 17. J. Halfvarson, C. J. Brislawn, R. Lamendella, Y. Vazquez-Baeza, W. A. Walters, L. M. Bramer, M. D'Amato, F. Bonfiglio, D. McDonald, A. Gonzalez, E. E. McClure, M. F. Dunkleberger, R. Knight and J. K. Jansson, Dynamics of the human gut microbiome in inflammatory bowel disease, *Nat Microbiol*, 2017, **2**, 17004.
 18. A. S. Meijnikman, V. E. Gerdes, M. Nieuwdorp and H. Herrema, Evaluating Causality of Gut Microbiota in Obesity and Diabetes in Humans, *Endocr Rev*, 2018, **39**, 133-153.
 19. K. H. Allin, V. Tremaroli, R. Caesar, B. A. H. Jensen, M. T. F. Damgaard, M. I. Bahl, T. R. Licht, T. H. Hansen, T. Nielsen, T. M. Dantoft, A. Linneberg, T. Jorgensen, H. Vestergaard, K. Kristiansen, P. W. Franks, I.-D. consortium, T. Hansen, F. Backhed and O. Pedersen, Aberrant intestinal microbiota in individuals with prediabetes, *Diabetologia*, 2018, **61**, 810-820.
 20. H. Chu, Y. Duan, L. Yang and B. Schnabl, Small metabolites, possible big changes: a microbiota-centered view of non-alcoholic fatty liver disease, *Gut*, 2019, **68**, 359-370.
 21. F. Z. Marques, C. R. Mackay and D. M. Kaye, Beyond gut feelings: how the gut microbiota regulates blood pressure, *Nat Rev Cardiol*, 2018, **15**, 20-32.
 22. C. L. Boulange, A. L. Neves, J. Chilloux, J. K. Nicholson and M. E. Dumas, Impact of the gut microbiota on inflammation, obesity, and metabolic disease, *Genome Med*, 2016, **8**, 42.
 23. L. J. Kasselmann, N. A. Vernice, J. DeLeon and A. B. Reiss, The gut microbiome and elevated cardiovascular risk in obesity and autoimmunity, *Atherosclerosis*, 2018, **271**, 203-213.
 24. Z. Jie, H. Xia, S. L. Zhong, Q. Feng, S. Li, S. Liang, H. Zhong, Z. Liu, Y. Gao, H. Zhao, D. Zhang, Z. Su, Z. Fang, Z. Lan, J. Li, L. Xiao, J. Li, R. Li, X. Li, F. Li, H. Ren, Y. Huang, Y. Peng, G. Li, B. Wen, B. Dong, J. Y. Chen, Q. S. Geng, Z. W. Zhang, H. Yang, J. Wang, J. Wang, X. Zhang, L. Madsen, S. Brix, G. Ning, X. Xu, X. Liu, Y. Hou, H. Jia, K. He and K. Kristiansen, The gut microbiome in atherosclerotic cardiovascular disease, *Nat Commun*, 2017, **8**, 845.
 25. Z. H. Shen, C. X. Zhu, Y. S. Quan, Z. Y. Yang, S. Wu, W. W. Luo, B. Tan and X. Y. Wang, Relationship between intestinal microbiota and ulcerative colitis: Mechanisms and clinical application of probiotics and fecal microbiota transplantation, *World J Gastroenterol*, 2018, **24**, 5-14.
 26. D. W. Kang, J. B. Adams, A. C. Gregory, T. Borody, L. Chittick, A. Fasano, A. Khoruts, E. Geis, J. Maldonado, S. McDonough-Means, E. L. Pollard, S. Roux, M. J. Sadowsky, K. S. Lipson, M. B. Sullivan, J. G. Caporaso and R. Krajmalnik-Brown, Microbiota Transfer Therapy alters gut ecosystem and improves gastrointestinal and autism symptoms: an open-label study, *Microbiome*, 2017, **5**, 10.
 27. C. J. Chang, C. S. Lin, C. C. Lu, J. Martel, Y. F. Ko, D. M. Ojcius, S. F. Tseng, T. R. Wu, Y. Y. Chen, J. D. Young and H. C. Lai, *Ganoderma lucidum* reduces obesity in mice by modulating the composition of the gut microbiota, *Nat Commun*, 2015, **6**, 7489.
 28. N. Khodaei and S. Karboune, Enzymatic generation of galactose-rich oligosaccharides/oligomers from potato rhamnogalacturonan I pectic polysaccharides, *Food Chem*, 2016, **197**, 406-414.
 29. A. J. Svagan, A. Kusic, C. De Gobba, F. H. Larsen, P. Sassene, Q. Zhou, M. van de Weert, A.

- Mullertz, B. Jorgensen and P. Ulvskov, Rhamnogalacturonan-I Based Microcapsules for Targeted Drug Release, *PLoS One*, 2016, **11**, e0168050. View Article Online
DOI: 10.1039/C9FO01534E
30. R. Di, M. S. Vakkalanka, C. Onumpai, H. K. Chau, A. White, R. A. Rastall, K. Yam and A. T. Hotchkiss, Jr., Pectic oligosaccharide structure-function relationships: Prebiotics, inhibitors of *Escherichia coli* O157:H7 adhesion and reduction of Shiga toxin cytotoxicity in HT29 cells, *Food Chem*, 2017, **227**, 245-254.
31. B. Gómez, B. Gullón, R. Yáñez, H. Schols and J. L. Alonso, Prebiotic potential of pectins and pectic oligosaccharides derived from lemon peel wastes and sugar beet pulp: A comparative evaluation, *Journal of Functional Foods*, 2016, **20**, 108-121.
32. S. Zhang, H. Hu, L. Wang, F. Liu and S. Pan, Preparation and prebiotic potential of pectin oligosaccharides obtained from citrus peel pectin, *Food Chem*, 2018, **244**, 232-237.
33. J. Li, S. Li, Y. Zheng, H. Zhang, J. Chen, L. Yan, T. Ding, R. J. Linhardt, C. Orfila, D. Liu, X. Ye and S. Chen, Fast preparation of rhamnogalacturonan I enriched low molecular weight pectic polysaccharide by ultrasonically accelerated metal-free Fenton reaction, *Food Hydrocolloids*, 2019, **95**, 551-561.
34. D. J. Strydom, Chromatographic separation of 1-phenyl-3-methyl-5-pyrazolone-derivatized neutral, acidic and basic aldoses, *Journal of Chromatography A*, 1994, **678**, 17-23.
35. D. W. Fadrosh, B. Ma, P. Gajer, N. Sengamalay, S. Ott, R. M. Brotman and J. Ravel, An improved dual-indexing approach for multiplexed 16S rRNA gene sequencing on the Illumina MiSeq platform, *Microbiome*, 2014, **2**, 6.
36. T. R. Wu, C. S. Lin, C. J. Chang, T. L. Lin, J. Martel, Y. F. Ko, D. M. Ojcius, C. C. Lu, J. D. Young and H. C. Lai, Gut commensal *Parabacteroides goldsteinii* plays a predominant role in the anti-obesity effects of polysaccharides isolated from *Hirsutella sinensis*, *Gut*, 2019, **68**, 248-262.
37. L. Zhang, X. Ye, T. Ding, X. Sun, Y. Xu and D. Liu, Ultrasound effects on the degradation kinetics, structure and rheological properties of apple pectin, *Ultrason Sonochem*, 2013, **20**, 222-231.
38. W. Burchard, Solution Properties of Branched Macromolecules, *Advances in polymer science*, 1999, **143**.
39. S. Podzimek, T. Vlcek and C. Johann, Characterization of branched polymers by size exclusion chromatography coupled with multiangle light scattering detector. I. Size exclusion chromatography elution behavior of branched polymers, *Journal of Applied Polymer Science*, 2001, **81**, 1588-1594.
40. G. Robinson, S. B. Ross-Murphy and E. R. Morris, Viscosity-molecular weight relationships, intrinsic chain flexibility, and dynamic solution properties of guar galactomannan, *Carbohydrate Research*, 1982, **107**, 17-32.
41. J. Wang and L. Zhang, Structure and chain conformation of five water-soluble derivatives of a beta-D-glucan isolated from *Ganoderma lucidum*, *Carbohydr Res*, 2009, **344**, 105-112.
42. A. N. Round, A. J. MacDougall, S. G. Ring and V. J. Morris, Unexpected branching in pectin observed by atomic force microscopy, *Carbohydrate Research*, 1997, **303**, 251-253.
43. M. Jin, S. Kalainy, N. Baskota, D. Chiang, E. C. Deehan, C. McDougall, P. Tandon, I. Martinez, C. Cervera, J. Walter and J. G. Abraldes, Faecal microbiota from patients with cirrhosis has a low capacity to ferment non-digestible carbohydrates into short-chain fatty acids, *Liver Int*, 2019.

44. X. Xu and X. Zhang, Lentinula edodes-derived polysaccharide alters the spatial structure of gut microbiota in mice, *PLoS One*, 2015, **10**, e0115037. View Article Online
DOI: 10.1039/C9FO01534E
45. P. Kungel, V. G. Correa, R. C. G. Correa, R. A. Peralta, M. Sokovic, R. C. Calhelha, A. Bracht, I. Ferreira and R. M. Peralta, Antioxidant and antimicrobial activities of a purified polysaccharide from yerba mate (*Ilex paraguariensis*), *Int J Biol Macromol*, 2018, **114**, 1161-1167.
46. E. Dahdouh, S. El-Khatib, E. Baydoun and R. M. Abdel-Massih, Additive Effect of MCP in Combination with Cefotaxime Against *Staphylococcus aureus*, *Med Chem*, 2017, **13**, 682-688.
47. T. Stalheim, S. Ballance, B. E. Christensen and P. E. Granum, Sphagnum--a pectin-like polymer isolated from Sphagnum moss can inhibit the growth of some typical food spoilage and food poisoning bacteria by lowering the pH, *J Appl Microbiol*, 2009, **106**, 967-976.
48. F. E. R. Michael A. M., Henning S., Peter J. T., Robert S. F., Characterizing a model human gut microbiota composed of members of its two dominant bacterial phyla, *PNAS*, 2009, **106**, 5859-5864.
49. G. P. Donaldson, S. M. Lee and S. K. Mazmanian, Gut biogeography of the bacterial microbiota, *Nat Rev Microbiol*, 2016, **14**, 20-32.
50. H. Zeng, C. Huang, S. Lin, M. Zheng, C. Chen, B. Zheng and Y. Zhang, Lotus Seed Resistant Starch Regulates Gut Microbiota and Increases Short-Chain Fatty Acids Production and Mineral Absorption in Mice, *J Agric Food Chem*, 2017, **65**, 9217-9225.
51. Y. Wang, N. Zhang, J. Kan, X. Zhang, X. Wu, R. Sun, S. Tang, J. Liu, C. Qian and C. Jin, Structural characterization of water-soluble polysaccharide from *Arctium lappa* and its effects on colitis mice, *Carbohydr Polym*, 2019, **213**, 89-99.
52. S. Hooda, B. M. Boler, M. C. Serao, J. M. Brule, M. A. Staeger, T. W. Boileau, S. E. Dowd, G. C. Fahey, Jr. and K. S. Swanson, 454 pyrosequencing reveals a shift in fecal microbiota of healthy adult men consuming polydextrose or soluble corn fiber, *J Nutr*, 2012, **142**, 1259-1265.
53. A. Salonen, L. Lahti, J. Salojarvi, G. Holtrop, K. Korpela, S. H. Duncan, P. Date, F. Farquharson, A. M. Johnstone, G. E. Lobley, P. Louis, H. J. Flint and W. M. de Vos, Impact of diet and individual variation on intestinal microbiota composition and fermentation products in obese men, *ISME J*, 2014, **8**, 2218-2230.
54. S. Leclercq, S. Matamoros, P. D. Cani, A. M. Neyrinck, F. Jamar, P. Starkel, K. Windey, V. Tremaroli, F. Backhed, K. Verbeke, P. de Timary and N. M. Delzenne, Intestinal permeability, gut-bacterial dysbiosis, and behavioral markers of alcohol-dependence severity, *Proc Natl Acad Sci U S A*, 2014, **111**, E4485-4493.
55. L. M. Cox, I. Cho, S. A. Young, W. H. Anderson, B. J. Waters, S. C. Hung, Z. Gao, D. Mahana, M. Bihan, A. V. Alekseyenko, B. A. Methe and M. J. Blaser, The nonfermentable dietary fiber hydroxypropyl methylcellulose modulates intestinal microbiota, *FASEB J*, 2013, **27**, 692-702.
56. S. Macfarlane, G. T. Macfarlane and J. H. Cummings, Review article: prebiotics in the gastrointestinal tract, *Aliment Pharmacol Ther*, 2006, **24**, 701-714.
57. S. Devriese, V. Eeckhaut, A. Geirnaert, L. Van den Bossche, P. Hindryckx, T. Van de Wiele, F. Van Immerseel, R. Ducatelle, M. De Vos and D. Laukens, Reduced Mucosa-associated *Butyricoccus* Activity in Patients with Ulcerative Colitis Correlates with Aberrant Claudin-1 Expression, *J Crohns Colitis*, 2017, **11**, 229-236.

58. E. C. Martens, E. C. Lowe, H. Chiang, N. A. Pudlo, M. Wu, N. P. McNulty, D. W. Abbott, B. Henrissat, H. J. Gilbert, D. N. Bolam and J. I. Gordon, Recognition and degradation of plant cell wall polysaccharides by two human gut symbionts, *PLoS Biol*, 2011, **9**, e1001221. View Article Online
DOI: 10.1039/C9FO01534E
59. D. Ndeh and H. J. Gilbert, Biochemistry of complex glycan depolymerisation by the human gut microbiota, *FEMS Microbiol Rev*, 2018, **42**, 146-164.
60. A. S. Luis, J. Briggs, X. Zhang, B. Farnell, D. Ndeh, A. Labourel, A. Basle, A. Cartmell, N. Terrapon, K. Stott, E. C. Lowe, R. McLean, K. Shearer, J. Schuckel, I. Venditto, M. C. Ralet, B. Henrissat, E. C. Martens, S. C. Mosimann, D. W. Abbott and H. J. Gilbert, Dietary pectic glycans are degraded by coordinated enzyme pathways in human colonic Bacteroides, *Nat Microbiol*, 2018, **3**, 210-219.
61. C. L. Karlsson, J. Onnerfalt, J. Xu, G. Molin, S. Ahrne and K. Thorngren-Jerneck, The microbiota of the gut in preschool children with normal and excessive body weight, *Obesity (Silver Spring)*, 2012, **20**, 2257-2261.
62. X. Jiao, Y. Wang, Y. Lin, Y. Lang, E. Li, X. Zhang, Q. Zhang, Y. Feng, X. Meng and B. Li, Blueberry polyphenols extract as a potential prebiotic with anti-obesity effects on C57BL/6 J mice by modulating the gut microbiota, *J Nutr Biochem*, 2019, **64**, 88-100.
63. D. M. Yunpeng Luan, Min Chen, , Structural changes of gut microbiota in mice with chronic constipation and intestinal tumor., 2017, **28**, 10062-10067.
64. T. Cerdo, J. A. Garcia-Santos, G. B. M and C. Campoy, The Role of Probiotics and Prebiotics in the Prevention and Treatment of Obesity, *Nutrients*, 2019, **11**.
65. S. Lim, D. H. Chang, S. Ahn and B. C. Kim, Whole genome sequencing of "Faecalibaculum rodentium" ALO17, isolated from C57BL/6J laboratory mouse feces, *Gut Pathog*, 2016, **8**, 3.
66. C. Onumpai, S. Kolida, E. Bonnin and R. A. Rastall, Microbial utilization and selectivity of pectin fractions with various structures, *Appl Environ Microbiol*, 2011, **77**, 5747-5754.
67. J. Chen, R. H. Liang, W. Liu, T. Li, C. M. Liu, S. S. Wu and Z. J. Wang, Pectic-oligosaccharides prepared by dynamic high-pressure microfluidization and their in vitro fermentation properties, *Carbohydr Polym*, 2013, **91**, 175-182.
68. T. Aljutaily, M. Consuegra-Fernandez, F. Aranda, F. Lozano and E. Huarte, Gut microbiota metabolites for sweetening type I diabetes, *Cell Mol Immunol*, 2018, **15**, 92-95.
69. Q. Shang, Y. Wang, L. Pan, Q. Niu, C. Li, H. Jiang, C. Cai, J. Hao, G. Li and G. Yu, Dietary Polysaccharide from Enteromorpha Clathrata Modulates Gut Microbiota and Promotes the Growth of Akkermansia muciniphila, Bifidobacterium spp. and Lactobacillus spp, *Mar Drugs*, 2018, **16**.
70. A. Koh, F. De Vadder, P. Kovatcheva-Datchary and F. Backhed, From Dietary Fiber to Host Physiology: Short-Chain Fatty Acids as Key Bacterial Metabolites, *Cell*, 2016, **165**, 1332-1345.
71. D. Rios-Covian, P. Ruas-Madiedo, A. Margolles, M. Gueimonde, C. G. de Los Reyes-Gavilan and N. Salazar, Intestinal Short Chain Fatty Acids and their Link with Diet and Human Health, *Front Microbiol*, 2016, **7**, 185.
72. J. H. Cummings, E. W. Pomare, W. J. Branch, C. P. Naylor and G. T. Macfarlane, Short chain fatty acids in human large intestine, portal, hepatic and venous blood, *Gut*, 1987, **28**, 1221-1227.
73. Q. Nie, J. Hu, H. Gao, L. Fan, H. Chen and S. Nie, Polysaccharide from Plantago asiatica L. attenuates hyperglycemia, hyperlipidemia and affects colon microbiota in type 2 diabetic rats,

- Food Hydrocolloids*, 2019, **86**, 34-42.
74. S. Y. Xu, J. J. Aweya, N. Li, R. Y. Deng, W. Y. Chen, J. Tang and K. L. Cheong, Microbial catabolism of *Porphyra haitanensis* polysaccharides by human gut microbiota, *Food Chem*, 2019, **289**, 177-186.
75. J. Gao, L. Lin, Z. Chen, Y. Cai, C. Xiao, F. Zhou, B. Sun and M. Zhao, In vitro digestion and fermentation of three polysaccharide fractions from *Laminaria japonica* and their impact on lipid metabolism-associated human gut microbiota, *J Agric Food Chem*, 2019, **67**(26): 7496-7505.
76. J. L. Hu, S. P. Nie, F. F. Min and M. Y. Xie, Polysaccharide from seeds of *Plantago asiatica* L. increases short-chain fatty acid production and fecal moisture along with lowering pH in mouse colon, *J Agric Food Chem*, 2012, **60**, 11525-11532.
77. P. B. Mortensen, K. Holtug and H. S. Rasmussen, Short-chain fatty acid production from mono- and disaccharides in a fecal incubation system: implications for colonic fermentation of dietary fiber in humans, *J Nutr*, 1988, **118**, 321-325.
78. Q. Shang, X. Shan, C. Cai, J. Hao, G. Li and G. Yu, Dietary fucoidan modulates the gut microbiota in mice by increasing the abundance of *Lactobacillus* and *Ruminococcaceae*, *Food Funct*, 2016, **7**, 3224-3232.
79. E. E. Canfora, J. W. Jocken and E. E. Blaak, Short-chain fatty acids in control of body weight and insulin sensitivity, *Nat Rev Endocrinol*, 2015, **11**, 577-591.
80. C. Di Lorenzo, C. M. Williams, F. Hajnal and J. E. Valenzuela, Pectin delays gastric emptying and increases satiety in obese subjects, *Gastroenterology*, 1988, **95**, 1211-1215.
81. C. Zhang, S. Li, L. Yang, P. Huang, W. Li, S. Wang, G. Zhao, M. Zhang, X. Pang, Z. Yan, Y. Liu and L. Zhao, Structural modulation of gut microbiota in life-long calorie-restricted mice, *Nat Commun*, 2013, **4**, 2163.

Figure captions:

Fig. 1. Primary structure of CP, WRP and DWRP. (A) FTIR spectra of the three pectin; (B) The ^1H NMR spectrum of the three pectin.

Fig. 2. Chain conformation of CP, WRP, and DWRP. Conformation plots of CP and WRP in 0.2 M aqueous NaCl solution at 25 °C. (A) The relationship between R_g and M_w , (B) Mark-Houwink-Sakurada equation; Representative topographical AFM images of (C) CP, (D) WRP and (E) DWRP

Fig. 3. Response of the cecal and colonic gut microbiota structure to CP, WRP and DWRP treatment. PCA score plot of cecal (A), 3D-PCoA of the cecal (B)

Fig. 4. Structural composition of gut microbiota among all mice groups. Cecal (a) microbiota in CD, CD-CP, CD-WRP and CD-DWRP groups at phylum level; cecal (b) microbiota in CD, CD-CP, CD-WRP and CD-DWRP groups at class level; cecal (c) microbiota in CD, CD-CP, CD-WRP and CD-DWRP groups at genus level.

Fig. 5. The taxonomic cladogram obtained from LEFse analysis of gut microbiota in different groups. Taxonomic cladogram of cecal microbiota in CD, CD-CP, CD-WRP and CD-DWRP groups

Fig. 6. The LDA score obtained from LEFse analysis of gut microbiota in different groups. A LDA effect size of more than 2.5 was used as a threshold for the LEFse analysis.

Fig. 7. The concentration ($\mu\text{mol/g}$) of acetic, propionate, butyrate, I-butyrate, valerate, and I-valerate in the cecal contents (A) and colon feces (B) of pectin treated group and chow diet group. * $P < 0.05$; ns, not significant.

Fig. 8. Growth performance (A) and weight gain (B) of mice in response to dietary CP, WRP and

DW/RP. *P<0.05.

View Article Online
DOI: 10.1039/C9FO01534E

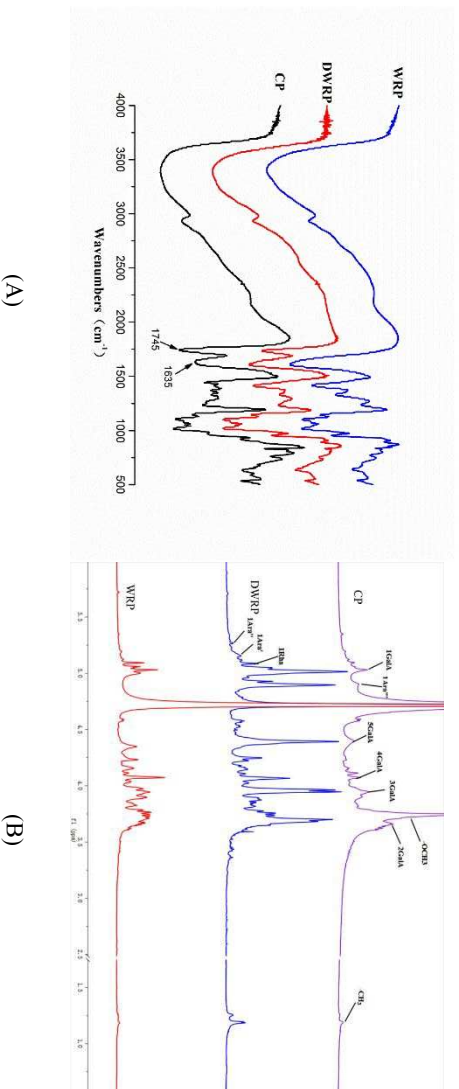


Fig. 1

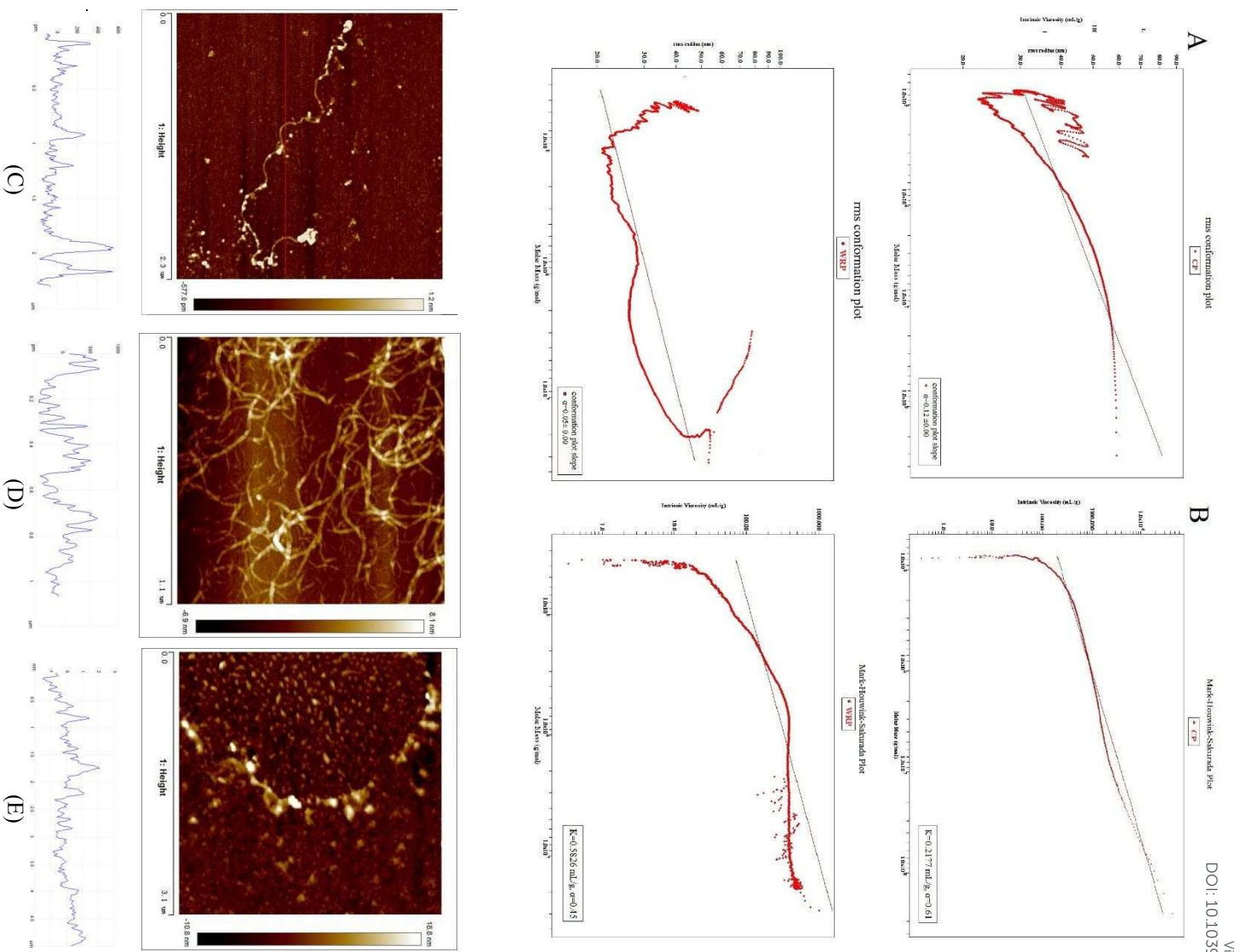


Fig. 2

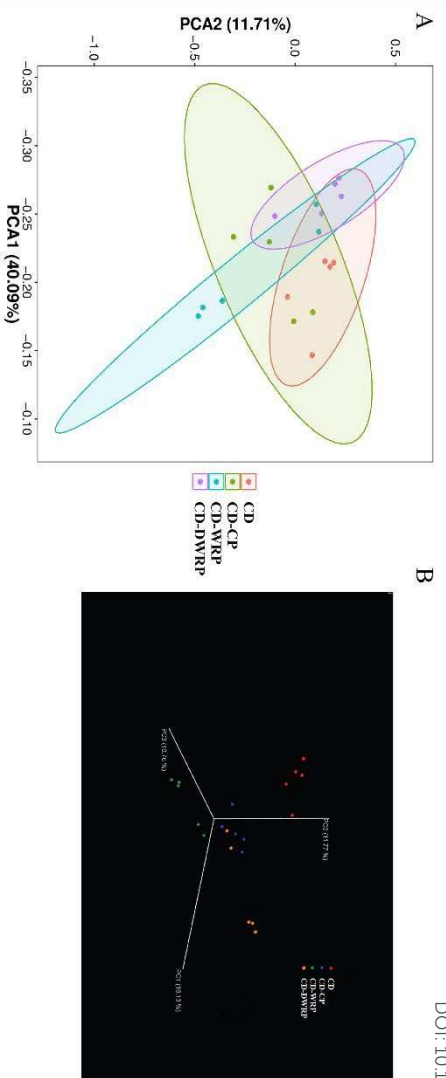


Fig. 3

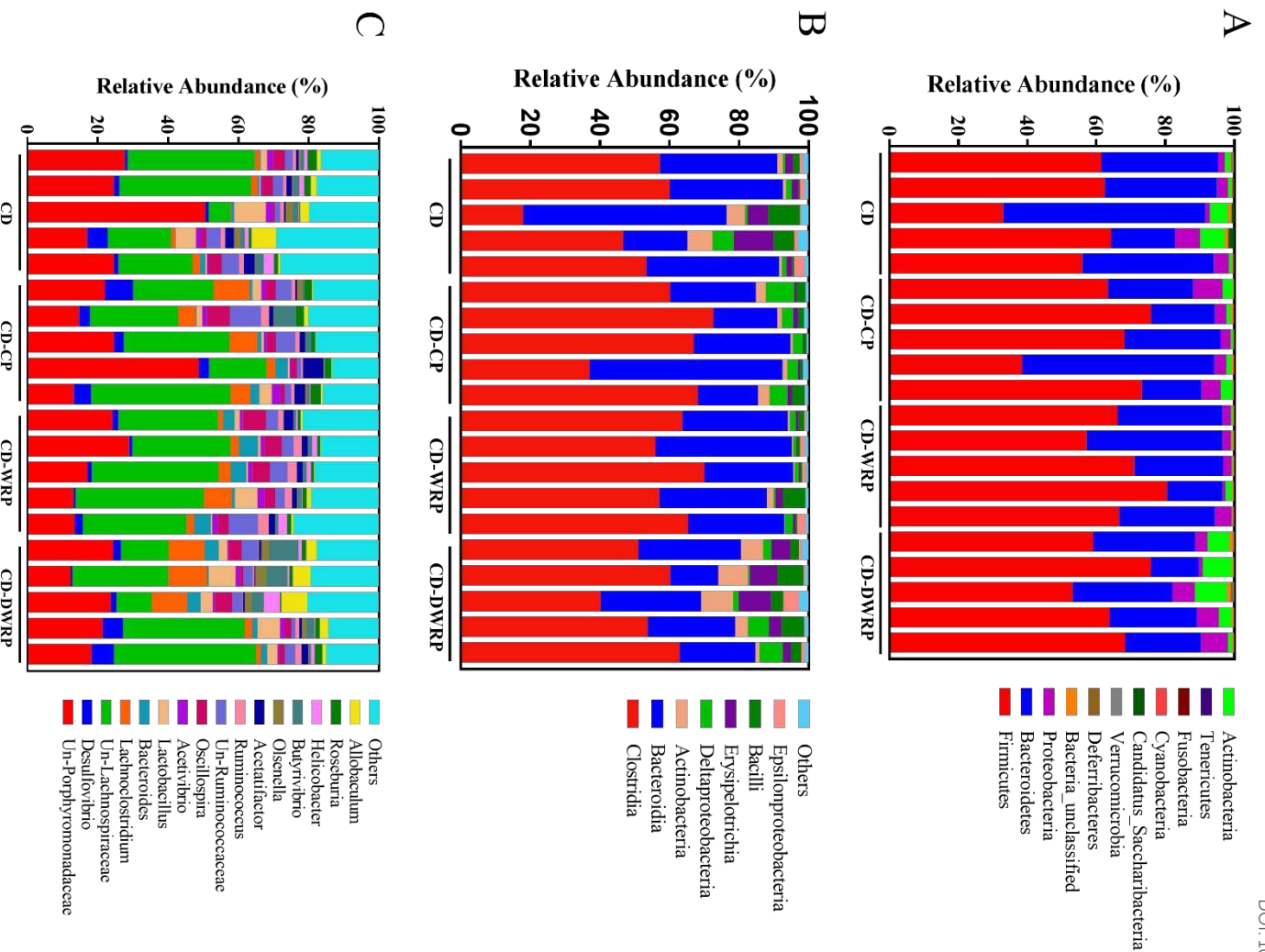


Fig. 4

Cladogram

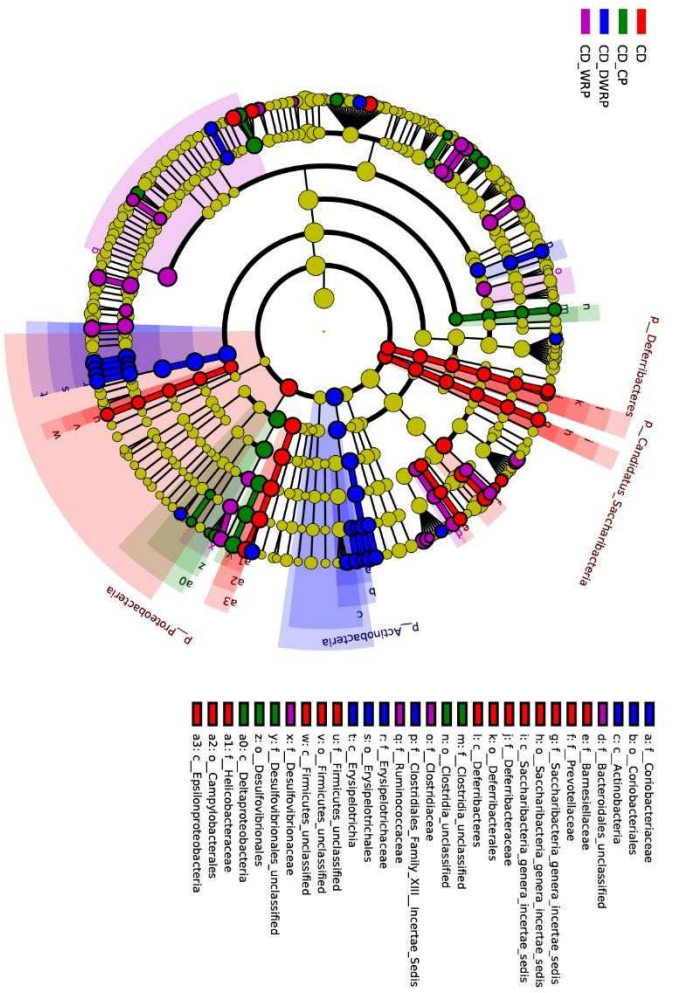


Fig. 5

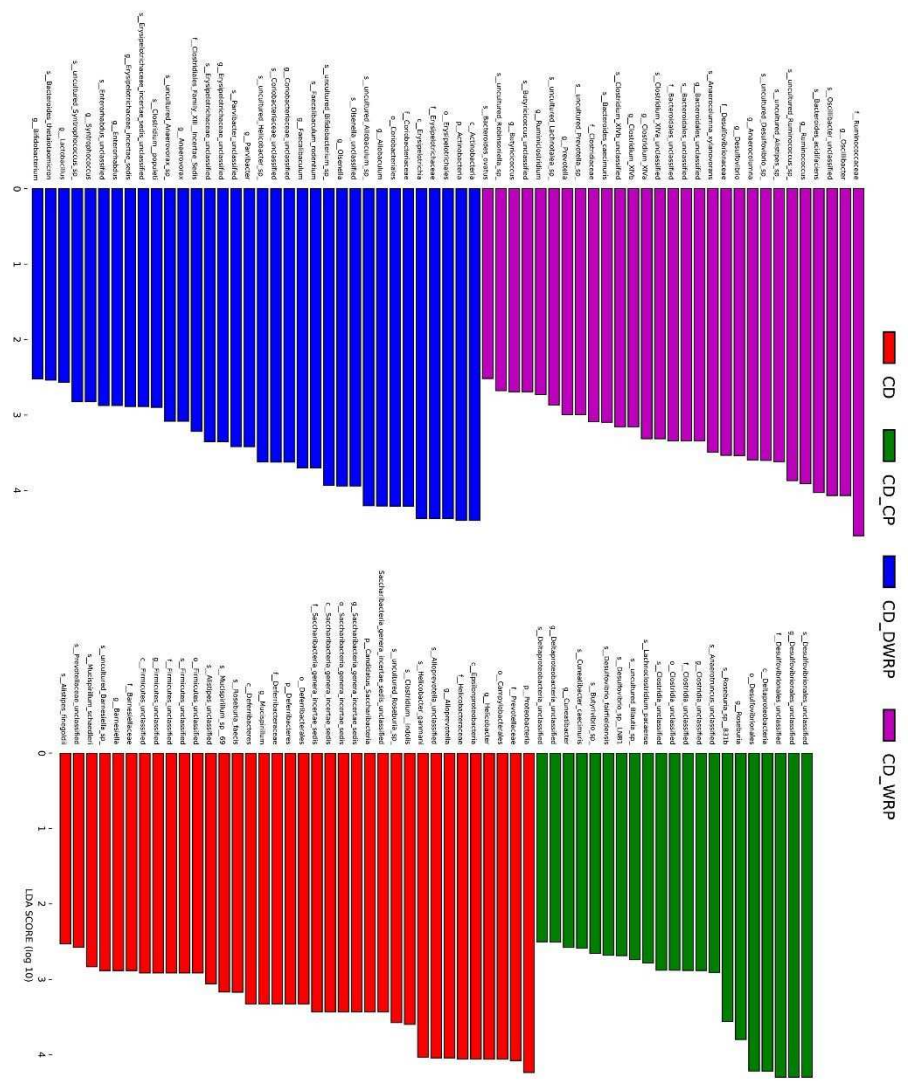
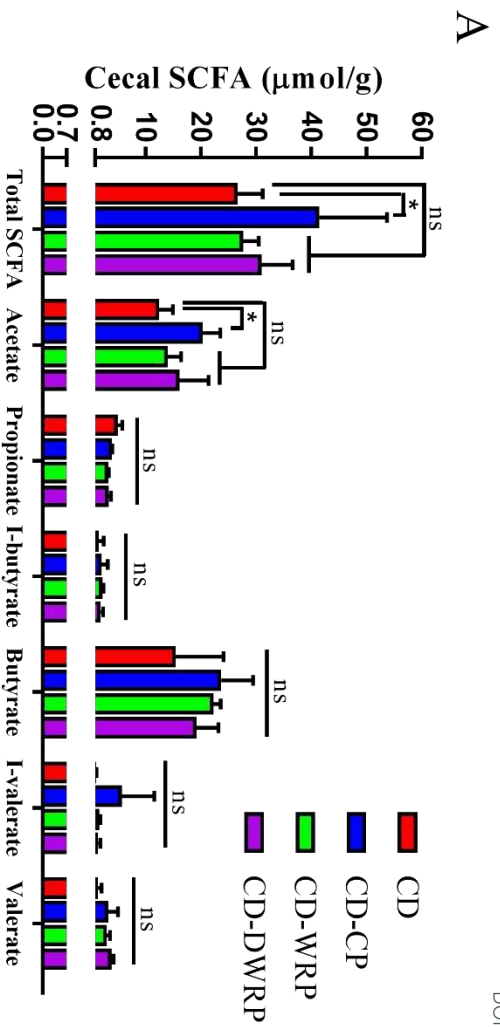


Fig. 6



View Article Online
DOI: 10.1039/C9FO01534E

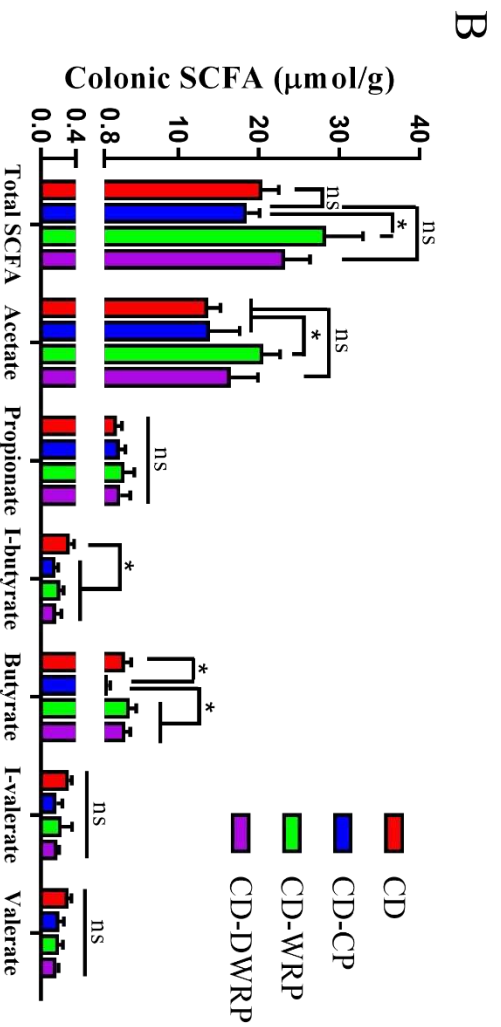


Fig. 7

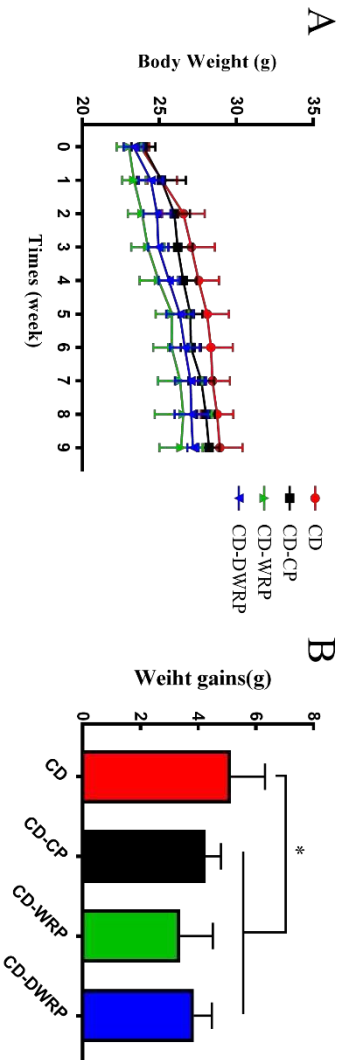


Fig. 8

Table 1. Monosaccharide compositions of CP, WRP and DWRP

Pectin	Molar ratio of monosaccharide								HG (%)	RG-I (%)	HG/RG-I	Rha:(Gal+Ara)
	Man	Rha	GluA	GalA	Glu	Gal	Ara	Fuc				
CP	0	4.45±0.38	0.37±0.02	56.99±0.69	10.15±0.03	13.03±0.12	13.84±0.14	0.20±0.02	52.55±1.07	35.77±1.02	1.47±0.07	1:6
WRP	2.16±0.17	3.61±0.16	0.25±0.01	28.64±0.85	0.75±0.06	14.27±0.16	48.94±0.81	1.37±0.16	25.03±0.98	70.44±1.22	0.36±0.02	1:20
DWRP	0	6.64±0.08	0.18±0.02	48.93±1.01	0.46±0.05	9.43±0.52	33.58±0.83	0.07±0.02	42.29±1.08	56.29±1.50	0.75±0.04	1:6

The molar percentage of homogalacturonan(HG) and rhamnogalacturonan of type I (RG-I) were calculated as the following formula:

$$\text{HG (\%)} = \text{GalA(mol\%)} - \text{Rha (mol\%)}$$

$$\text{RG-I (\%)} \approx 2\text{Rha(mol\%)} + \text{Ara(mol\%)} + \text{Gal(mol\%)}$$

The Rha:(Gal+Ara) ratio stands for the degree of the side chain branching.

Table 2. The abundance of key phylotypes of gut microbiota modulated by dietary CP, WRP and DWRP in CD-fed mice

View Article Online
DOI: 10.1039/C9FO01534E

Key Phylotypes	CD	CD-CP	CD-WRP	CD-DWRP
<i>g_Bifidobacterium</i>	0.87±1.32 ^{ab}	0.44±0.33 ^a	0.26±0.37 ^a	2.09±1.83 ^b
<i>g_Lactobacillus</i>	1.64±2.27 ^a	1.70±1.15 ^a	2.34±2.03 ^a	4.46±2.03 ^b
<i>g_Faecalibaculum</i>	0.37±0.36 ^a	0.06±0.05 ^a	0.03±0.02 ^a	1.05±0.67 ^b
<i>g_Bacteroides</i>	0.55±0.53 ^a	1.62±1.34 ^{ab}	2.85±2.14 ^b	2.27±1.49 ^{ab}
<i>g_Ruminococcus</i>	1.12±0.22 ^a	1.21±0.69 ^a	2.34±0.57 ^b	0.72±0.64 ^a
<i>f_Ruminococcaceae</i>	1.10±0.61 ^a	12.68±7.17 ^{bc}	17.58±3.32 ^c	9.97±2.41 ^b
<i>g_Clostridium_XIVa</i>	0.12±0.12 ^a	0.31±0.30 ^{ab}	0.48±0.30 ^b	0.17±0.16 ^{ab}
<i>g_Desulfovibrio</i>	0.24±0.17 ^a	0.14±0.06 ^a	0.78±0.34 ^b	0.21±0.11 ^a

Data representing relative abundance (the percentage of bacteria) of the key phylotypes of gut microbiota are expressed as the mean ± SD (n=6). The means with different superscript represent statistically significant results ($p < 0.05$) based on one-way analysis of variance (ANOVA) with Duncan's range tests, whereas means labeled with the same superscript correspond to results that show no statistically significant differences

Graphical abstract:View Article Online
DOI: 10.1039/C9FO01534E

Rhamnogalacturonan-I (RG-I) pectin (WRP) with high neutral sugar side chain was recovered from citrus segment membrane. The present study reveals that WRP can stimulate the growth of beneficial microbiome, improving SCFA content. Besides, the effect could be enhanced by free-radical depolymerizing of WRP into DWRP.

